J. Water Environ. Nanotechnol., 5(4): 307-320 Autumn 2020

ORIGINAL RESEARCH PAPER

Facile Green Synthesis of Silver Doped ZnO Nanoparticles Using *Tridax* Procumbens Leaf Extract and their Evaluation of Antibacterial Activity

A.Ubaithulla Baig[1*], R. Vadamalar[1], A. Vinodhini[2], S. Fairose[3], A. Gomathiyalini[4], N. Jabena Begum[2], Shaista Jabeen[2]

[1] PG and Research Department of Physics, Muthurangam Government Arts College, Vellore, India
[2] PG and Research Department of Zoology, DKM College for Women (A), Vellore, India
[3] Department of Physics, AIMAN College of Arts and Science for Women, Trichy, India
[4] PG and Research Department of Physics, H.H. The Rajah's College, Pudukkottai, India
[5] Department of Physics, DKM College for Women (A), Vellore, India

Received: 2020-08-16 Accepted: 2020-10-21 Published: 2020-11-15

ABSTRACT

Silver and zinc oxide are well known for both their antimicrobial and pro-healing properties. ZnO is a biocompatible and bio-safe material that possesses photo-oxidizing and photo-catalysis impacts on chemical and biological species. ZnO nanomaterials could interact chemically as well as physically in order to exhibit antibacterial activities. Chemical interactions of the ZnO nanomaterials with bacterial cells leads to the photo-induced production of reactive oxygenated species (ROS), formation of H_2O_2, and the release of Zn^{2+} ions. In contrast, physical interaction could show biocidal effects through cell envelope rupturing, cellular internalization, or mechanical damage. In this article, we present a green method using Tridax Procumbens leaf extract to synthesize Ag-doped ZnO nanoparticles (NPs) in order to explore the synergistic antibacterial properties of Ag and ZnO nanoparticles against certain gram-positive and gram-negative bacterial strains. The newly synthesized Ag-doped ZnO NPs were characterized by X-ray diffraction (XRD) in order to study the crystalline structure, composition, and purity. Transmission electron microscopy (TEM), Scanning electron microscopy (SEM) and Dynamic Light Scattering (DLS) techniques were used to study particle size, shape, and morphology. The XRD and UV studies confirmed the ZnO phase. The absorbance peak around 618 cm^{-1}- 749 cm^{-1} in the FTIR spectrum referred to the presence of silver. The surface morphological studies also supported the FTIR result. The synthesized sample exhibited enhanced antibacterial activity irrespective of all tested microorganisms than the standard antibiotic used. The maximum size distribution of particles is found to be around 60 nm from the DLS technique.

Keywords: *Zinc Oxide nanoparticles, Green synthesis, Tridax Procumbens, Antibacterial Study, Gram-positive, and gram-negative bacteria*

How to cite this article
Ubaithulla Baig. A., Vadamalar R., Vinodhini A., Fairose S., Gomathiyalini A., Jabena Begum N., Shaista Jabeen. Facile Green Synthesis of Silver Doped ZnO Nanoparticles Using Tridax Procumbens Leaf Extract and their Evaluation of Antibacterial Activity. J. Water Environ. Nanotechnol., 2020; 5(4): 307-320.
DOI: 10.22090/jwent.2020.04.002

INTRODUCTION

Growing awareness of health and hygiene in recent years has emanated in an aggressive increase in the demand for antimicrobial agents as it is the breakthrough for the major issue of bacterial contamination. Various inorganic metal oxides have the potentiality for therapeutics, diagnostics, surgical device coatings, and nanomedicine applications. Among the metal oxides, Zinc Oxide (ZnO) is gaining attention in the last decade owing to its selective toxicity in biological systems [1]. As

* Corresponding Author Email: *baig.ubaidulla@gmail.com*

Table 1: Literature survey on ZnO based NPs synthesized from various plant sources

Sl. No	Precursor	Leaf of Plant	Studied Microbes for Antimicrobial Activity	References
1.	Zinc Acetate Dihydrate	Green Tea	S.Aureus, Aspergillus Niger	[16]
2.	Zinc Acetate Dihydrate	CoriandrumSativum	E.Coli	[17]
3.	Zinc Acetate Dihydrate	AnisochillusCarnosus, AzadEracta Indica	Aspergillus Niger, Pseudomonoans Aeruginosa	[18]
4.	Zinc Acetate Dihydrate	Aloe Barbadensis	E.Coli, S.Aureus	[19]
5.	Zinc Nitrate	Coptidis Rhizoma	E.Coli, Bacillus Megaterium, Bacillus Pumillus	[20]
6.	Zinc Acetate Dihydrate	Eryngium Foetidum	E.Coli, S.Aureus, Pseudomonas Aeruginosa	[21]
7.	Zinc Nitrate Hexahydrate	Pongamia Pinnata	E.Coli, S.Aureus	[22]
8.	Zinc Nitrate Hexahydrate	Moringa Oleifera	S.Aureus, E.Coli, Proteus Mirabilis Candida Albicans, Candida Tropicalis	[23]
9.	Zinc Nitrate	Solanum Nigrum	E.Coli, S.Aureus, Vibrio Cholerae	[24]
10.	Zinc Nitrate Hexahydrate	Cassia Fistula	Klebsilla Aerogenus, Pseudomonas Desmolyticum, E.Coli, S.Aureus	[25]
11.	Zinc Acetate Dihydrate	Glycosmis Pentaphylla	S.Aureus, Shigella Dysentrea, Salmonella Paratyphy, Aspergillus Niger, Candida Albicans	[26]
12.	Zinc Acetate	Psidium Guajava	S.Aureus, E.Coli	[27]
13.	Zinc Nitrate Hexahydrate	Tabernaemontana Divaricata	S.Aureus, E.Coli	[28]
14.	Zinc Nitrate Hexahydrate	Mentha Pulegium	S.Aureus, E.Coli	[29]
15.	Zinc Chloride, Silver Chloride (ZnO:Ag)	Justicia Adhatoda	S.Aureus, E.Coli	[30]
16.	Zinc Nitrate Hexahydrate	Euphorbia Heterophylla	E.Coli, S.Aureus, Pseudmonas Desmolyticum, Klebsilla Aerogenes	[31]
17.	Zinc Acetate	Acalypha Indica	E.Coli, S.Aureus	[32]
18.	Zinc Acetate Dihydrate,	AzadEracta Indica	S.Aureus, E.Coli, Streptococcus Progenes	[33]
19.	Zinc Oxide	Cinnamomum Tamala	S.Aureus	[34]

the bandgap of ZnO is 3.37 eV and the excitation binding energy is 60 meV at room temperature, it is considered to be a promising material for optoelectronic devices, transparent conducting, piezoelectric, and photo-degradation (i.e. waste water treatment)applications [2-6]. Moreover, according to USFDA (US Food and Drug Administration), ZnO is considered as a non-toxic and low-cost material [7]. In addition, ZnO nanoparticles (NPs) have also been proposed as an antimicrobial preservative for wood and food products [8].

In recent days, not only the selection of material which is non-toxic and low cost is to be considered, but also the synthesis method having less toxicity, as well as cost-effectiveness, plays a vital role in the development of newer material suitable for health care technology.

Keeping aforesaid points in mind, in the present study silver doped ZnO nanoparticles (NPs) were synthesized using the green approach. It is well known that the green approach for the synthesis of NPs has the possibility of the least utilization of chemicals, low cost, and low energy requirement [9, 10]. Currently, the green synthesis of NPs using plants is emerging as a newer branch of nanotechnology due to its cost-effectiveness and eco-friendly alternative [11-15].

According to the literature survey, various research communities have synthesized ZnO based NPs from various plant sources and have been studied for its antimicrobial activity as reported in Table 1[16-34]. In the present work, the leaf of *Tridax procumbens* has been used to prepare silver doped ZnO NPs (ZnO: Ag NPs). To the best of our knowledge, this is the first work on the synthesis of ZnO: Ag nanoparticles using *Tridax procumbens* leaf extract.

Tridax procumbens, a plant belonging to the daisy family is one of the most common plants

used by rural and tribal communities in order to cure various health ailments. This plant habitats, waste places, roadsides, and hedges throughout India. Several reports from tribal areas in India state that the leaf extract of *Tridax procumbens* could be used to treat fresh wounds, stop bleeding, and also operate as a hair tonic [35-37]. In addition to this, *Tridax procumbens* is reported to have anti-inflammatory, immune modulator, anti-diabetic, hemostatic, antioxidant, hepatoprotective, antipyretic, and antimicrobial activity [38-40].

In the present investigation, the synthesis of ZnO: Ag NPs has a two-step procedure: First, the bio-reduction of silver nitrate by *Tridax procumbens* leaf extract using broth method and secondly, the preparation of ZnO: Ag NPs using a simple soft chemical route. These two methods have been proposed as cost-effective and the present study would be an environmentally friendly alternative to the chemical and physical methods. Hence, we have synthesized ZnO: Ag NPs via a green approach for antibacterial screening against certain gram-negative and gram-positive bacteria which will support the development of the disinfectant technology.

MATERIALS AND METHODS

Green synthesis of silver (Ag) nanoparticles

The silver nanoparticles were prepared using the broth method employed by Shankar et al. for the synthesis of Ag nanoparticles using Geranium leaf extract [41]. In the present study,, fresh and healthy leaves of *Tridax procumbens* were collected from the Vellore District having latitude of 12.9165 N and 79.1325 E, during December 2019. The collected leaves were washed with Purified Milli-Q water in order to remove the unwanted impurities and dust particles and thereafter they were dried with filter paper to remove any drops of water from the leaves. 1 gm of the leaf was weighed and mixed with 100 ml of distilled water in a conical flask and boiled for 5 min. After cooling, the leaf extract was filtered with Whatman No.1 filter paper. To the 100 ml of the leaf extract, 1mM of Silver Nitrate ($AgNO_3$) was added and mixed nicely and was kept at room temperature for 5 minutes. The color change (greenish-yellow color changed to dark brown) was observed after 5min of the addition of Silver Nitrate to the plant extract which indicates the formation of silver nanoparticles.

Preparation of green synthesized ZnO: Ag NPs

ZnO: Ag NPs were synthesized by a simple soft chemical route. 0.2 M of zinc acetate dihydrate [$Zn(CH_3COO)_2{\cdot}2H_2O$] dissolved in 4:1 (i.e. 160 mL:40 mL) ratio of H_2O and the prepared plant extract (with silver NPs) is treated as the starting solution (200mL). A suitable amount of ammonium hydroxide pellets (NH_4OH) were added to maintain the pH level ≈ 8 of the starting solution. The obtained mixture is stirred for 2h under the temperature of 85 °C. The product is filtered, washed, and then calcined at 500 °C for 2h using Muffle Furnace (Model: Thermolyne benchtop muffle furnace (F48025-60)-duty 1200 °C). Subsequently, the final product is taken for further characterization.

Characterization of the synthesized sample

The crystalline structure of the green synthesized NPs was studied using the X-ray powder diffraction technique (PANalytical-PW 340/60 X' pert PRO) using CuK_a radiation (λ = 0.15406 nm). The UV absorption spectrum is recorded using PerkinElmer (Lambda 750) UV-Vis-NIR spectrophotometer. Fourier transforms infrared (FTIR) spectrum was recorded using the PerkinElmer RX-I FTIR spectrophotometer employing the KBr technique. The surface morphology of the synthesized ZnO: Ag NPs was observed using a scanning electron microscope (Carl Zeiss Ultra 55 FE-SEM). The microstructure of the Phyto-mediated Ag-doped ZnO NPs was analyzed using a transmission electron microscope (TEM, Hitachi H-7100). The size of the synthesized particles was measured using a particle size analyzer (Micromeritics, Nano Plus model).

Antimicrobial Assay

The antimicrobial activity of green synthesized ZnO: Ag NPs was tested against six different bacteria using the agar well diffusion method. For bacterial growth, Mueller Hinton Broth is used as a nutrient agar medium. This agar medium contains beef extract, peptone, sodium chloride, and yeast. Later on, the prepared medium was sterilized in an autoclave at 120 °C for 20 min, and subsequently, it was poured into a sterile petri dish and was allowed to solidify in a laminar airflow chamber. After solidification, by using a sterile cotton swab, fresh bacterial culture was spread over the plate

using a spread plate technique. Three wells were bored into the plates using a sterile cork borer of 5 mm in diameter one each for control, for standard antibiotic Nitrofurantoin, and for stock solution having the synthesized sample (300 µg/mL). After loading the wells, the bacterial plates were incubated at 37 °C for 24 hr. Later on, the plates were monitored for the clear inhibition zone around the well. The diameter of the inhibition zone was measured in mm. In the present study, three-gram positive bacterial cultures namely *Staphylococcus aureus, Streptococcus pyogenes, and Bacillus subtilis,* and three-gram negative bacterial cultures namely *Escherichia coli, Klebsiella pneumonia,* and *Pseudomonas aeruginosa* were used as test microbes.

RESULTS AND DISCUSSION

Structural Studies

The characterization of the crystalline material and the evaluation of the crystal structure, crystal orientation, and crystal defects can be studied using XRD analytical technique. The XRD pattern of green synthesized ZnO: Ag NPs is shown in Fig. 1a. This XRD pattern exhibits the diffraction peaks at ≈32°, 34°, 36°, 47°, 56°, 63°, 66°and 68° corresponding to (100), (002), (101), (102), (110), (103), (200) and (112), respectively. The observed peaks indicate the wurtzite crystalline structure and hexagonal phase of ZnO which are relevant to those in the ZnO standard powder diffraction file JCPDS card no.: 00-036-1451.

From this XRD pattern, it is obvious that there is no significant peak for Ag related phases or any considerable shift in the location of the diffraction peaks as compared with standard ZnO. This implies that the lattice structure of the ZnO crystal has not significantly changed by the incorporation of biosynthesized silver nanoparticles into the ZnO lattice.

Using the following Debye-Scherrer's formula [42, 43] the crystallite size (D) of the NPs was calculated:

$$D = \frac{k\lambda}{\beta cos\theta} \quad (1)$$

Where k is a constant equal to 0.90, λ is the wavelength of the incident X-rays, β is the full width at half maximum (FWHM) in radian, and θ is the Bragg's angle in radian. The calculated value of the crystallite size is found to be 50 nm. This is similar to the previous literature where ZnO NPs

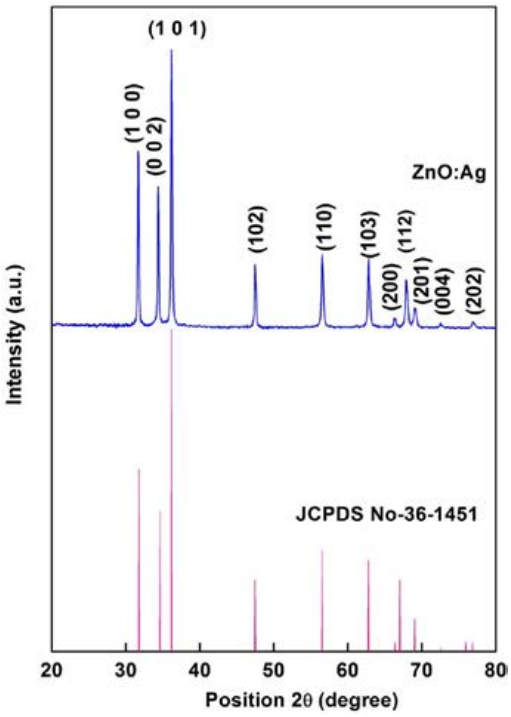

Figure 1a

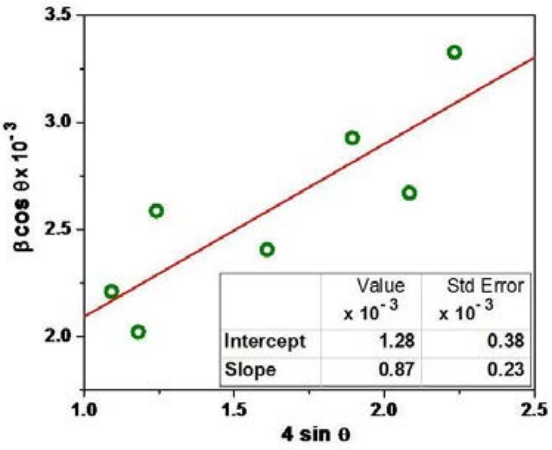

Figure 1b

Fig. 1. a: XRD pattern of ZnO:Ag nanoparticles synthesized using Tridax Procumbens leaf extract. b:Typical Williamson-Hall plot for the estimation of crystallite size of green synthesized ZnO:Ag nanoparticles

synthesized using Costus pictus leaf extract [44] is having a crystallite size of 29.11 nm, and the work related to Mentha pulegium leaf extract mediated synthesis of ZnO NPs reports a crystallite size of 44.94 nm [29]. Another literature where ZnO NPs have been synthesized using Anisochilus carnosus

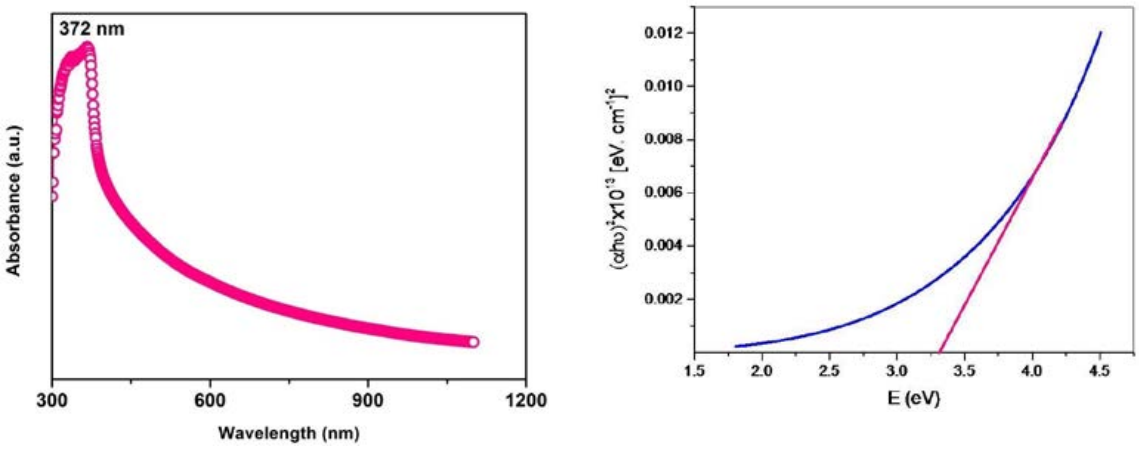

a b

Fig. 2. a: Absorption spectrum of ZnO:Ag nanoparticles synthesized using Tridax Procumbens leaf extract
b: Tauc's plot obtained by absorption spectrum of green synthesized ZnO:Ag nanopartilces

leaf extract also indicated similar lattice structures obtained in the XRD pattern of the ZnO NPs and it reports various sizes which include 56.14, 49.55, and 38.59 nm, for 30, 40, and 50 ml of extract addition, respectively [15]. Hence, it is believed that the addition of phytochemicals plays a vital role in enhancing the crystalline nature of ZnO.

In addition to these, the crystallite size was also calculated from the Williamson-Hall (W-H) plot. This helps to evaluate the size and strain component of the peak broadening simultaneously unlike the conventional Debye-Scherrer's equation. Furthermore, it enables *h k l*-dependent broadening and crystallite shape prediction (Transformation from Conducting Ferromagnetic to diamagnetic insulator). W-H equation [45-48] is given below:

$$\beta \cos\theta = \left(\frac{k\lambda}{D}\right) + \left(4\varepsilon \sin\theta\right) \quad (2)$$

Where the notations β, θ, λ, D, and k have their usual meaning as explained in the previous section and ε refers to induced lattice strain. From the W-H plot (Fig. 1b), the estimated values of crystallite size and lattice strain are found to be 108 nm and ~ 0.1 % respectively. The crystallite size estimated from the W-H plot (108 nm) is found to be more than that of the D-S (50 nm) method which emphasizes the role of the induced lattice strain in the prepared ZnO: Ag nanoparticles. Such a difference in the value of crystallite size estimated from these two methods has been reported in the literature [49, 50].

Optical Studies

Fig. 2a shows the absorption spectrum of the biosynthesized ZnO: Ag NPs recorded in the range of 300–1000 nm. The absorption peak obtained at 372 nm is due to their large excitation binding energy of ZnO at room temperature [51]. This absorption edge peak at 372 nm implies the blue-shift of the synthesized ZnO NPs compared with its bulk counterpart (377 nm) which is owing to it to the quantum confinement effect [52, 53]. A similar shift was obtained in previous literature in which ZnO NPs have been synthesized using Laurus nobilis [54], Solanum torvum [55], Ixora coccinea [56], and Parthenium hysterophorus [8], leaf extracts with the absorption edge in the range of 340–375 nm, confirming the narrow particle size distribution [57]. In the present study, due to this quantum confinement effect, the obtained band gap (3.33 eV) is higher as compared with the bulk ZnO (3.29 eV).

The bandgap energy of ZnO nanoparticles is calculated using Tauc's plot using the formula given below [58-60]:

$\alpha = (1/d)\, A\ (cm^{-1})$ (3)

Where d, is the sample cell thickness, (cm)
A is the absorbance (arb. unit)
α is the absorbance coefficient, (cm^{-1})

$\alpha h\upsilon = (h\upsilon - E_g)^n$ (4)

where E_g is the bandgap of the material, (eV)
h is Planks Constant (6.626×10^{-34} Js),
υ is the frequency given by (c/ λ), (Hz)
c is the velocity of light (3×10^8 m/s)

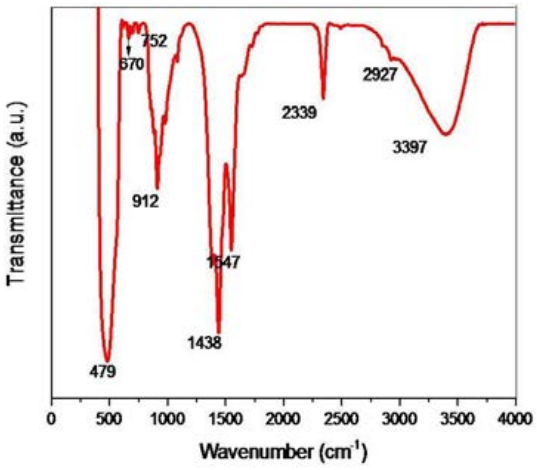

Fig. 3: FTIR spectrum of ZnO:Ag nanoparticles synthesized using Tridax Procumbens leaf extract

and n is the exponent which depends on the type of the bandgap

The bandgap energy calculated using Tauc's plot (Fig. 2b) is found to be 3.3 eV.

FTIR studies

The FTIR spectrum of ZnO: Ag nanoparticles is shown in Fig. 3. These particles indicated a broad peak at 3397 cm^{-1} which could be attributed to the characteristic absorption of the hydroxyl group and the peak at 479 cm^{-1} is formed due to the absorption of Zn-O bonds [61]**.** The peak near 2927 cm^{-1} is assigned to the alkyne group present in the phytoconstituents of the *Tridax procumbens* leaf extract [62]. The peak around 600 cm^{-1} to 800 cm^{-1} refers to silver [63]**.** Hence, the observed smaller peaks near 618 cm^{-1} - 749 cm^{-1}, confirm the incorporation of silver NPs into the ZnO lattice. Furthermore, the peak around 700 cm^{-1} is responsible for the presence of emodin [64] which is a bioactive compound derived from the *Tridax procumbens* leaf extract in the sample. The other peaks around 1300-1400 cm^{-1} are responsible for the presence of NO_2 symmetric stretching which is also due to the presence of leaf extract in the starting solution. Hence, the observed FTIR results indicate that the green synthesized silver nanoparticles are incorporated into the ZnO lattice and are in agreement with the literature. In addition, certain other phytochemicals of the *Tridax procumbens* leaf extract were also identified from the spectrum.

Dynamic Light Scattering (DLS) Analysis

DLS technique is widely used in order to identify the particle size distribution of the nanoparticles. Fig. 4 indicates that the distribution of particle size for the phytomediated silver doped ZnO NPs is from 40 to 120 nm with the maximum size distribution is around 60 nm. From this result, it is assumed that the phytochemicals of the leaf extract present in the starting solution influence the particle size of the ZnO NPs to be in the nano range.

SEM and TEM Analyses

The SEM image of the ZnO: Ag NPs is shown in Fig. 5. This SEM micrograph shows that most of the nanoparticles are in a hexagon shape which is the basic structure of ZnO and spherical shaped nanoparticles are also observed. In addition to this, certain nano-stick-like structures are also observed (inset of Fig. 5) indicating that Ag enters into the ZnO lattice and influences the morphology of the synthesized samples [30]. Moreover, these ZnO: Ag NPs exhibit uniform morphology with certain voids. These voids play a vital role in exhibiting enhanced antimicrobial activity [65] as evidenced by the forthcoming section (Antimicrobial analysis).

The transmission electron micrograph of the phytomediated ZnO: Ag NPs is shown in Fig. 6. This image reveals that most of the nanoparticles are spherical and their diameter is found to be around 18 to 22 nm. The particles are also shown to be quasi-spherical and hexagonal shaped. In addition to this, certain nanoparticles exhibit a nano-stick-like structure as evidenced by the inset of Fig. 6. It is in good agreement with the surface morphology recorded by the SEM technique.

It is well known that SEM is used for

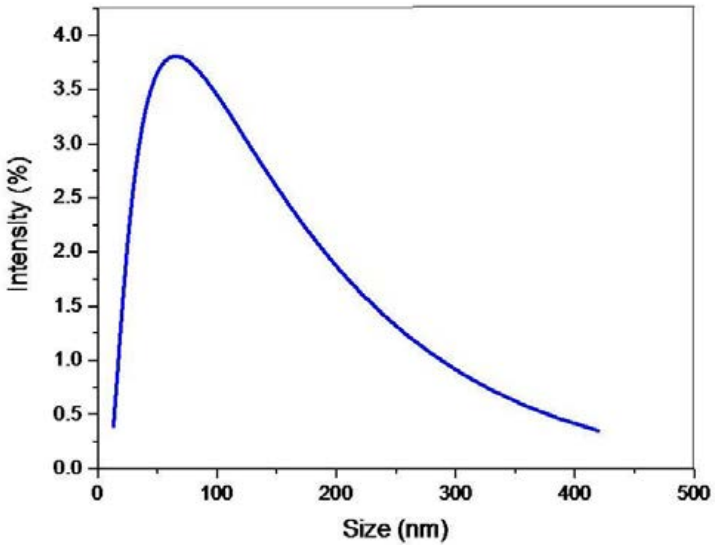

Fig. 4: DLS analysis of ZnO:Ag nanoparticles synthesized using Tridax Procumbens leaf extract

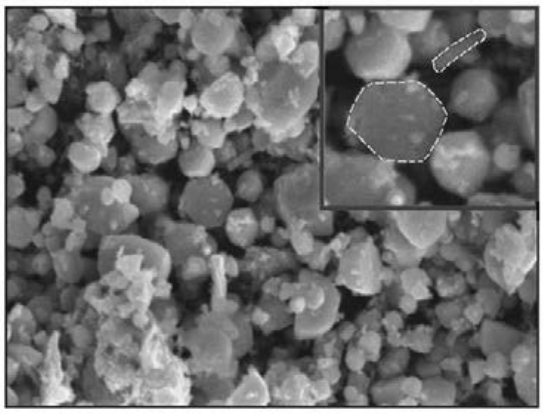

Fig. 5: SEM image of ZnO:Ag nanoparticles synthesized using Tridax Procumbens leaf extract

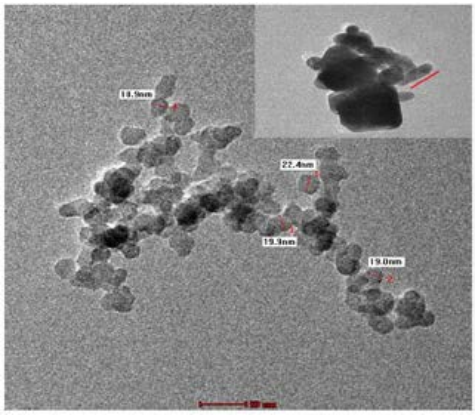

Fig. 6: TEM image of ZnO:Ag nanoparticles synthesized using Tridax Procumbens leaf extract

imaging the surface of the nanoparticle on a submicroscopic scale. In contrast, the use of TEM is to image the internal structure of the particle on a nanometer scale. Hence, the particles appear ~3% larger in the SEM than in the TEM microscope. In the present study, the average particle size is observed to be ~20 nm from the TEM image whereas the SEM image is ~55 nm. The formation of these smaller sized (~20 nm) nanoparticles are the ones responsible for boosting up the antibacterial activity of the green synthesized ZnO: Ag NPs.

Antibacterial Studies

The antibacterial activity of Ag-doped ZnO NPs was examined for gram-positive bacteria like *Staphylococcus aureus, Streptococcus pyogenes, and Bacillus subtilis,* and gram-negative bacteria like *Escherichia coli, Klebsiella pneumonia,* and *Pseudomonas aeruginosa,* and their impacts are shown in Fig 7 a and b, respectively. From these figures, it is obvious that the green synthesized Ag-doped ZnO NPs exhibit a remarkable antibacterial activity against all six foodborne pathogens as denoted by the zone diameter of inhibition in mm. Fig. 8a shows the inhibitory efficacy of the green synthesized ZnO: Ag NPs against gram-positive bacteria over the standard antibiotic used; whereas Fig. 8b shows for gram-negative bacteria over the standard antibiotic used. Although the

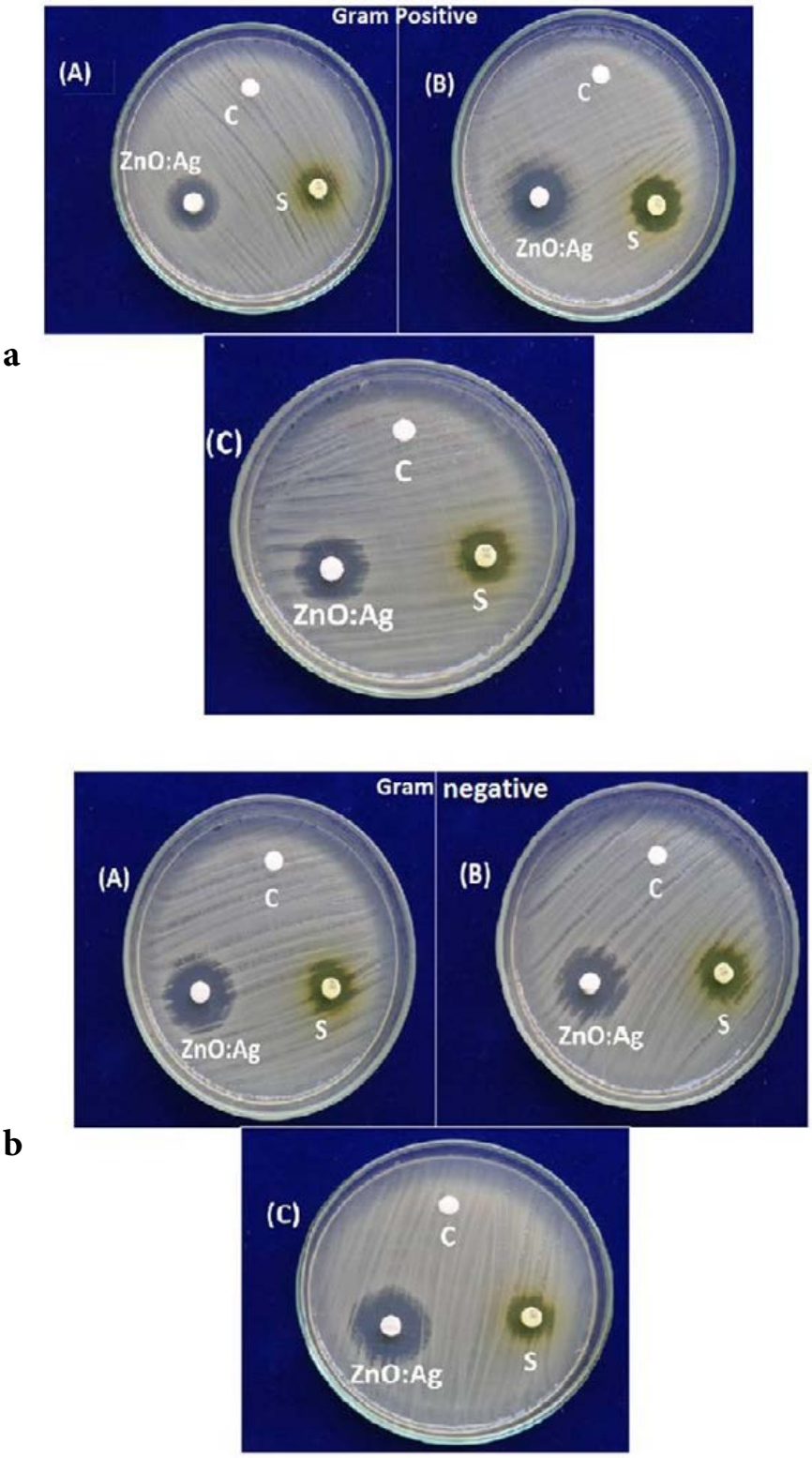

Fig. 7. a: Photos of agar plates inoculated with gram positive bacteria a) *Staphylococcus aureus* b) *Streptococcus pyogenes* and c) *Bacillus subtilis* together with green synthesized ZnO:Ag NPs

b: Photos of agar plates inoculated with gram negative bacteria a) *Escherichia coli*, b) *Klebsiella pneumonia* and c) *Pseudomonas aeruginosa* together with green synthesized ZnO:Ag NPs

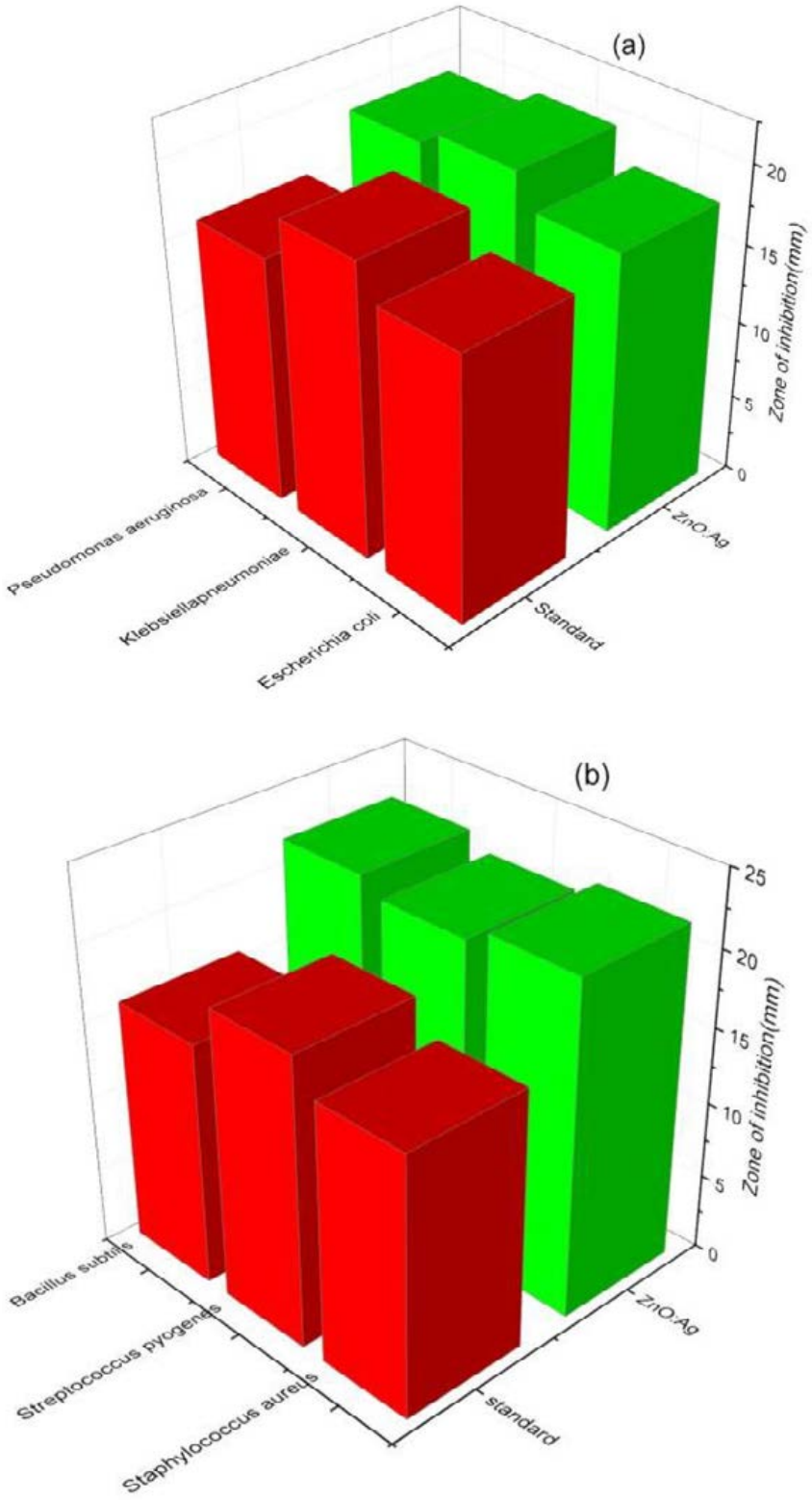

Fig. 8. a. The inhibitory efficacy of green synthesized ZnO:Ag NPs against gram positive bacteria
b. The inhibitory efficacy of green synthesized ZnO:Ag NPs against gram negative bacteria

synthesized sample shows enhanced antibacterial activity against all the tested bacteria, it exhibits comparatively higher efficiency against gram-positive bacteria than gram-negative bacteria which could be understood from the bar diagram represented in Fig. 8 a and b. The present findings are in good agreement with the reports given by various researchers working with different leaf extract based ZnO NPs [66, 67] and their reports suggest that this phenomenon may be attributed to the difference in the cell wall structures of the gram-negative and positive bacteria. As the gram-positive bacteria have a less complicated cell wall structure compared to gram-negative bacteria it is easy for the toxicants (here it is ZnO: Ag NPs) to access the sites of action for rupturing the cell structure which leads to death of it.

Some researchers observed lesser antibacterial activity for green synthesized ZnO based NPs when compared to a standard tablet used [15, 68-71]. But contrary to their results, in the present study, we observed higher antibacterial activity for the green synthesized ZnO: Ag NPs as compared to the standard antibiotic used (Nitrofurantoin) which may be due to the smaller/reduced particle sizes (~20 nm) of the synthesized nanoparticles which provides more surface area to interact with microbes, resulting in enhanced antimicrobial activity. It is well known that the antibacterial efficacy of ZnO NPs was inversely proportional to the size of nanoparticles [72]. From the literature survey, it is inferred that the green synthesized ZnO NPs exhibit better antibacterial activity when compared with the chemically synthesized ZnO NPs and are even with simple/bare plant extracts [68,73, 74].

As it is already well known, the antibacterial mechanism of Ag and ZnO NPs is having the following sequence: i) release of Ag^{+} and Zn^{2+} ions, ii) direct attachment of these ions onto cell surfaces, and iii) production of reactive oxygen species (ROS) to attack the bacterial cell as consequence apoptosis of it [75-77].

In addition to these, the enhanced antibacterial activity of the synthesized sample is due to the presence of certain phytochemicals of the *Tridax procumbens* leaf extract in it. Some of the research groups [78-80] subjected the *Tridax procumbens* leaf extract for qualitative phytochemical screening to identify the presence of chemical constituents like Steroids, Saponin, Alkaloids, Phenol, proteins, emodins, amino acids, etc., Among these, emodin is found to be a highly bioactive compound. Based on its in-vivo studies it is proved to have therapeutic potential like Strong Anti-inflammatory, antioxidant, cardiovascular, CNS, Antineoplastic agent, metabolic, hepato-protective, respiratory, anti-microbial, laxative, and immune-modulator. From this literature survey, it is believed that the presence of emodin in our synthesized sample will also play a role in enhancing the antibacterial efficacy. The presence of emodin could be identified from the FTIR spectrum Sec. 3.3. Thus in this case aforesaid factors are combined in order to work together for damaging the bacteria and as a consequence, enhancing the antibacterial efficacy of the synthesized sample.

CONCLUSION

To summarize, Ag-doped ZnO NPs were synthesized by an ecofriendly green approach using *Tridax procumbens* leaf extract. The XRD pattern illustrated that the synthesized sample has hexagonal structure of ZnO. The crystallite size calculated from the Scherrer method was found to be 50 nm whereas using Williamson-Hall method was found to be 108 nm along with the lattice strain 0.81×10^{-3}. FTIR spectrum and the surface morphological (SEM & TEM) studies confirmed the presence of Ag into the ZnO lattice. The excellent synergic antibacterial properties of the newly synthesized Ag-doped ZnO NPs was observed for gram-positive and gram-negative bacteria. It was observed that Ag-doped ZnO NPs exhibited comparatively higher antibacterial activity when compared to the standard antibiotic Nitrofurantoin; this was due to the smaller particle size with the presence of the phytochemicals of *Tridax procumbens* leaf, mainly Emodin. The presence of emodin was also confirmed by the FTIR studies. This is an advancement over traditional treatment methods as maximum bacterial strains have developed multiple antibiotic resistances toward commonly used antibiotic drugs.

FUNDING

The authors received no specific funding for this work.

CONFLICT OF INTEREST

The authors declare that they have no conflict of interest.

REFERENCES

1. Elumalai K, Velmurugan S, Ravi S, Kathiravan V, Adaikala Raj G. Bio-approach: Plant mediated synthesis of ZnO nanoparticles and their catalytic reduction of methylene blue and antimicrobial activity. Advanced Powder Technology. 2015;26(6):1639-51.
2. Divband B., Jodaei A and Khatamian M, 2019. Enhancement of photocatalytic degradation of 4-nitrophenol by integrating Ag nanoparticles with ZnO/HZSM-5 nanocomposite. Iranian J. Catalysis, 9(1): 63–70.
3. Bahrami M, Nezamzadeh-Ejhieh A. Effect of supporting and hybridizing of FeO and ZnO semiconductors onto an Iranian clinoptilolite nano-particles and the effect of ZnO/FeO ratio in the solar photodegradation of fish ponds waste water. Materials Science in Semiconductor Processing. 2014;27:833-40.
4. Khodami Z, Nezamzadeh-Ejhieh A. Investigation of photocatalytic effect of ZnO–SnO2/nano clinoptilolite system in the photodegradation of aqueous mixture of 4-methylbenzoic acid/2-chloro-5-nitrobenzoic acid. Journal of Molecular Catalysis A: Chemical. 2015;409:59-68.
5. Shirzadi A, Nezamzadeh-Ejhieh A. Enhanced photocatalytic activity of supported CuO–ZnO semiconductors towards the photodegradation of mefenamic acid aqueous solution as a semi real sample. Journal of Molecular Catalysis A: Chemical. 2016;411:222-9.
6. Nezamzadeh-Ejhieh A, Bahrami M. Investigation of the photocatalytic activity of supported ZnO–TiO2on clinoptilolite nano-particles towards photodegradation of wastewater-contained phenol. Desalination and Water Treatment. 2014;55(4):1096-104.
7. Vijayakumar S, Mahadevan S, Arulmozhi P, Sriram S, Praseetha PK. Green synthesis of zinc oxide nanoparticles using Atalantia monophylla leaf extracts: Characterization and antimicrobial analysis. Materials Science in Semiconductor Processing. 2018;82:39-45.
8. Rajiv P, Rajeshwari S, Venckatesh R. Bio-Fabrication of zinc oxide nanoparticles using leaf extract of Parthenium hysterophorus L. and its size-dependent antifungal activity against plant fungal pathogens. Spectrochimica Acta Part A: Molecular and Biomolecular Spectroscopy. 2013;112:384-7.
9. Sharmila G, Thirumarimurugan M, Muthukumaran C. Green synthesis of ZnO nanoparticles using Tecoma castanifolia leaf extract: Characterization and evaluation of its antioxidant, bactericidal and anticancer activities. Microchemical Journal. 2019;145:578-87.
10. Sharmila G, Haries S, Farzana Fathima M, Geetha S, Manoj Kumar N, Muthukumaran C. Enhanced catalytic and antibacterial activities of phytosynthesized palladium nanoparticles using Santalum album leaf extract. Powder Technology. 2017;320:22-6.
11. Taghavi Fardood S., Ramazani A and Woo Joo S, 2017. Sol-gel Synthesis and Characterization of Zinc Oxide Nanoparticles Using Black Tea Extract. J. App. Chem. Res, 11(4):8-17.
12. Taghavi Fardood S., Moradnia F., Mostafaei M., Afshari Z., Faramarzi V and Ganjkhanlu S (2019) Biosynthesis of MgFe2O4 magnetic nanoparticles and its application in photo-degradation of malachite green dye and kinetic study. Nanochem Res, 4(1): 86–93.
13. Taghavi Fardood S, Forootan R, Moradnia F, Afshari Z, Ramazani A. Green synthesis, characterization, and photocatalytic activity of cobalt chromite spinel nanoparticles. Materials Research Express. 2020;7(1):015086.
14. Moradnia F, Taghavi Fardood S, Ramazani A, Gupta VK. Green synthesis of recyclable MgFeCrO4 spinel nanoparticles for rapid photodegradation of direct black 122 dye. Journal of Photochemistry and Photobiology A: Chemistry. 2020;392:112433.
15. Anbuvannan M, Ramesh M, Viruthagiri G, Shanmugam N, Kannadasan N. Anisochilus carnosus leaf extract mediated synthesis of zinc oxide nanoparticles for antibacterial and photocatalytic activities. Materials Science in Semiconductor Processing. 2015;39:621-8.
16. Irshad S, Salamat A, Anjum AA, Sana S, Saleem RS, Naheed A, et al. Green tea leaves mediated ZnO nanoparticles and its antimicrobial activity. Cogent Chemistry. 2018;4(1).
17. Surya Pratap Goutam., Anil Kumar Yadav and Amar Jyoti Das, 2017. Coriander Extract Mediated Green Synthesis of Zinc Oxide Nanoparticles and their Structural, Optical and Antibacterial Properties. J. Nanosci. Tech, 3:249-252.
18. Agarwal H, Venkat Kumar S, Rajeshkumar S. A review on green synthesis of zinc oxide nanoparticles – An eco-friendly approach. Resource-Efficient Technologies. 2017;3(4):406-13.
19. Shakeel Ahmed., Annu., Saif AliChaudry and Saiqalkram, 2017. ZnO nanoparticles using plant extracts and microbes: A prospect towards green chemistry. J. Photochem. Photobiol. B, 166:272-284.
20. Nagajyothi PC, Sreekanth TVM, Tettey CO, Jun YI, Mook SH. Characterization, antibacterial, antioxidant, and cytotoxic activities of ZnO nanoparticles using Coptidis Rhizoma. Bioorganic & Medicinal Chemistry Letters. 2014;24(17):4298-303.
21. Begum S, Ahmaruzzaman M, Adhikari PP. Ecofriendly bio-synthetic route to synthesize ZnO nanoparticles using Eryngium foetidum L. and their activity against pathogenic bacteria. Materials Letters. 2018;228:37-41.
22. Ambika S and Sundrarajan M, 2017. Synthesis of zinc oxide nanoparticles using plant leaf extract against urinary tract infection pathogen. J. Adv. Pow. Tech, 3:459-465.
23. Elumalai K, Velmurugan S, Ravi S, Kathiravan V, Ashokkumar S. RETRACTED: Facile, eco-friendly and template free photosynthesis of cauliflower like ZnO nanoparticles using leaf extract of Tamarindus indica (L.) and its biological evolution of antibacterial and antifungal activities. Spectrochimica Acta Part A: Molecular and Biomolecular Spectroscopy. 2015;136:1052-7.
24. Ramesh M, Anbuvannan M, Viruthagiri G. Green synthesis of ZnO nanoparticles using Solanum nigrum leaf extract and their antibacterial activity. Spectrochimica Acta Part A: Molecular and

Biomolecular Spectroscopy. 2015;136:864-70.
25. Suresh D, Nethravathi PC, Udayabhanu, Rajanaika H, Nagabhushana H, Sharma SC. Green synthesis of multifunctional zinc oxide (ZnO) nanoparticles using Cassia fistula plant extract and their photodegradative, antioxidant and antibacterial activities. Materials Science in Semiconductor Processing. 2015;31:446-54.
26. Vijayakumar S, Krishnakumar C, Arulmozhi P, Mahadevan S, Parameswari N. Biosynthesis, characterization and antimicrobial activities of zinc oxide nanoparticles from leaf extract of Glycosmis pentaphylla (Retz.) DC. Microbial Pathogenesis. 2018;116:44-8.
27. Saha R, Subramani K, Petchi Muthu Raju SAK, Rangaraj S, Venkatachalam R. Psidium guajava leaf extract-mediated synthesis of ZnO nanoparticles under different processing parameters for hydrophobic and antibacterial finishing over cotton fabrics. Progress in Organic Coatings. 2018;124:80-91.
28. Raja A, Ashokkumar S, Pavithra Marthandam R, Jayachandiran J, Khatiwada CP, Kaviyarasu K, et al. Eco-friendly preparation of zinc oxide nanoparticles using Tabernaemontana divaricata and its photocatalytic and antimicrobial activity. Journal of Photochemistry and Photobiology B: Biology. 2018;181:53-8.
29. Rad SS, Sani AM, Mohseni S. Biosynthesis, characterization and antimicrobial activities of zinc oxide nanoparticles from leaf extract of Mentha pulegium (L.). Microbial Pathogenesis. 2019;131:239-45.
30. Pandiyan N, Murugesan B, Arumugam M, Sonamuthu J, Samayanan S, Mahalingam S. Ionic liquid - A greener templating agent with Justicia adhatoda plant extract assisted green synthesis of morphologically improved Ag-Au/ZnO nanostructure and it's antibacterial and anticancer activities. Journal of Photochemistry and Photobiology B: Biology. 2019;198:111559.
31. Lingaraju K, Naika HR, Nagabhushana H, Nagaraju G. Euphorbia heterophylla (L.) mediated fabrication of ZnO NPs: Characterization and evaluation of antibacterial and anticancer properties. Biocatalysis and Agricultural Biotechnology. 2019;18:100894.
32. Karthik S, Siva P, Balu KS, Suriyaprabha R, Rajendran V, Maaza M. Acalypha indica– mediated green synthesis of ZnO nanostructures under differential thermal treatment: Effect on textile coating, hydrophobicity, UV resistance, and antibacterial activity. Advanced Powder Technology. 2017;28(12):3184-94.
33. Bhuyan T, Mishra K, Khanuja M, Prasad R, Varma A. Biosynthesis of zinc oxide nanoparticles from Azadirachta indica for antibacterial and photocatalytic applications. Materials Science in Semiconductor Processing. 2015;32:55-61.
34. Agarwal H, Nakara A, Menon S, Shanmugam V. Eco-friendly synthesis of zinc oxide nanoparticles using Cinnamomum Tamala leaf extract and its promising effect towards the antibacterial activity. Journal of Drug Delivery Science and Technology. 2019;53:101212.
35.Mundada S and Shivhare R, 2010. Pharmacology of Tridax procumbens a Weed, Review. Inter. J. Pharm Tech Res, 2(2):1391-1394.
36. Perumal Samy R, Ignacimuthu S, Raja DP. Preliminary screening of ethnomedicinal plants from India. Journal of Ethnopharmacology. 1999;66(2):235-40.
37.Zambare AV., Chakraborthy GS and Banerjee SK, 2010. **Pharmacognostic Studies of Potential Herb –** *Tridax Procumbens* **Linn.** Inter. J. Pharm Sci. Res, 1(9):58-62.
38. Salami SA, Salahdeen HM, Rahman OC, Murtala BA, Raji Y. Oral administration of Tridax procumbens aqueous leaf extract attenuates reproductive function impairments in L-NAME induced hypertensive male rats. Middle East Fertility Society Journal. 2017;22(3):219-25.
39.Suseela L., Sarsvathy A and Brindha P, 2002. Pharmacognostic studies on Tridax procumbens L. (Asteraceae). J. Phytol. Res, 5(2):141–147.
40. Taddei A, Rosas-Romero AJ. Bioactivity studies of extracts from Tridax procumbens. Phytomedicine. 2000;7(3):235-8.
41. Shankar SS, Ahmad A, Sastry M. Geranium Leaf Assisted Biosynthesis of Silver Nanoparticles. Biotechnology Progress. 2003;19(6):1627-31.
42. Zhang T, Zhang Y, Jiang H, Wang X. Adjusting the pore size of nano-cellulose aerogel by heat treatment in the gel stage. Materials Research Express. 2019;6(7):075027.
43. Atrak K, Ramazani A, Taghavi Fardood S. Eco-friendly synthesis of Mg0.5Ni0.5AlxFe2-xO4 magnetic nanoparticles and study of their photocatalytic activity for degradation of direct blue 129 dye. Journal of Photochemistry and Photobiology A: Chemistry. 2019;382:111942.
44. Suresh J, Pradheesh G, Alexramani V, Sundrarajan M, Hong SI. Green synthesis and characterization of zinc oxide nanoparticle using insulin plant (Costus pictus D. Don) and investigation of its antimicrobial as well as anticancer activities. Advances in Natural Sciences: Nanoscience and Nanotechnology. 2018;9(1):015008.
45.Balakrishnan M and John R, 2020. Properties of sol-gel synthesized multiphase TiO2 (Ab)-ZnO (Zw) semiconductor nanostructure: An effective catalyst for methylene blue dye degradation. Iranian J. Catalysis, 10(1):1–16.
46. Omrani N, Nezamzadeh-Ejhieh A. Focus on scavengers' effects and GC-MASS analysis of photodegradation intermediates of sulfasalazine by Cu2O/CdS nanocomposite. Separation and Purification Technology. 2020;235:116228.
47. Chahkandi M, Arami SRS, Mirzaei M, Mahdavi B, Hosseini-Tabar SM. A new effective nano-adsorbent and antibacterial material of hydroxyapatite. Journal of the Iranian Chemical Society. 2018;16(4):695-705.
48. Tamiji T, Nezamzadeh-Ejhieh A. Electrocatalytic behavior of AgBr NPs as modifier of carbon past electrode in the presence of methanol and ethanol in aqueous solution: A kinetic study. Journal of the Taiwan Institute of Chemical Engineers. 2019;104:130-8.
49. Kibasomba PM, Dhlamini S, Maaza M, Liu C-P, Rashad MM, Rayan DA, et al. Strain and grain size of TiO2 nanoparticles from TEM, Raman spectroscopy and XRD: The revisiting of the Williamson-Hall plot method. Results in Physics. 2018;9:628-35.
50. Mohammed Gazzali PM, Rajan S, Chandrasekaran

G. Transformation from conducting ferromagnetic to insulating diamagnetic in vanadium doped ZnO nanoparticles. Journal of Materials Science: Materials in Electronics. 2017;29(1):823-36.
51.Sukanta Pal., Sourav Mondal., Jayanta Maity and Ratul Mukherjee, 2018. Synthesis and Characterization of ZnO Nanoparticles using Moringa Oleifera Leaf Extract: Investigation of Photocatalytic and Antibacterial Activity. Int. J. Nanosci. Nanotech, 149(2):111-119.
52. Bohren CF, Huffman DR. Absorption and Scattering of Light by Small Particles: Wiley; 1998 1998/04/23.
53. Mikhailov MM, Neshchimenko VV, Li C, Vlasov VA. Blue shift in absorption edge of polycrystalline zinc oxide modified by nanoparticles before and after irradiation exposure. Nuclear Instruments and Methods in Physics Research Section B: Beam Interactions with Materials and Atoms. 2018;418:18-26.
54. Fakhari S, Jamzad M, Kabiri Fard H. Green synthesis of zinc oxide nanoparticles: a comparison. Green Chemistry Letters and Reviews. 2019;12(1):19-24.
55. Ezealisiji KM, Siwe-Noundou X, Maduelosi B, Nwachukwu N, Krause RWM. Green synthesis of zinc oxide nanoparticles using Solanum torvum (L) leaf extract and evaluation of the toxicological profile of the ZnO nanoparticles–hydrogel composite in Wistar albino rats. International Nano Letters. 2019;9(2):99-107.
56. Yedurkar S, Maurya C, Mahanwar P. Biosynthesis of Zinc Oxide Nanoparticles Using Ixora Coccinea Leaf Extract—A Green Approach. Open Journal of Synthesis Theory and Applications. 2016;05(01):1-14.
57. Khorsand Zak A, Razali, Abd Majid WHB, Darroudi M. Synthesis and characterization of a narrow size distribution of zinc oxide nanoparticles. International Journal of Nanomedicine. 2011:1399.
58.Dianat S, 2018. Visible light induced photocatalytic degradation of direct red 23 and direct brown 166 by InVO4-TiO2 nanocomposite. Iranian J. Catalysis 8(2):121–132.
59. Derikvandi H, Nezamzadeh-Ejhieh A. Comprehensive study on enhanced photocatalytic activity of heterojunction ZnS-NiS/zeolite nanoparticles: Experimental design based on response surface methodology (RSM), impedance spectroscopy and GC-MASS studies. Journal of Colloid and Interface Science. 2017;490:652-64.
60. Babaahamdi-Milani M, Nezamzadeh-Ejhieh A. A comprehensive study on photocatalytic activity of supported Ni/Pb sulfide and oxide systems onto natural zeolite nanoparticles. Journal of Hazardous Materials. 2016;318:291-301.
61. Akhil K, Jayakumar J, Gayathri G, Khan SS. Effect of various capping agents on photocatalytic, antibacterial and antibiofilm activities of ZnO nanoparticles. Journal of Photochemistry and Photobiology B: Biology. 2016;160:32-42.
62. Malini S, Vignesh Kumar S, Hariharan R, Pon Bharathi A, Renuka Devi P, Hemananthan E. Antibacterial, photocatalytic and biosorption activity of chitosan nanocapsules embedded with Prosopis juliflora leaf extract synthesized silver nanoparticles. Materials Today: Proceedings. 2020;21:828-32.
63. Asnaashari Kahnouji Y, Mosaddegh E, Bolorizadeh MA. Detailed analysis of size-separation of silver nanoparticles by density gradient centrifugation method. Materials Science and Engineering: C. 2019;103:109817.
64. Saito ST, Silva G, Pungartnik C, Brendel M. Study of DNA–emodin interaction by FTIR and UV–vis spectroscopy. Journal of Photochemistry and Photobiology B: Biology. 2012;111:59-63.
65. Brown D. Antibiotic resistance breakers: can repurposed drugs fill the antibiotic discovery void? Nature Reviews Drug Discovery. 2015;14(12):821-32.
66.Arora K, 2015. Comparative account of allelopathic potential of different parts of Cassia occidentalis and its correlation with bio-molecular profile through FTIR. J. Chem. Pharm. Research, 7(12):91–95.
67. Vijayakumar S, Vaseeharan B, Malaikozhundan B, Shobiya M. Laurus nobilis leaf extract mediated green synthesis of ZnO nanoparticles: Characterization and biomedical applications. Biomedicine & Pharmacotherapy. 2016;84:1213-22.
68. Gunalan S, Sivaraj R, Rajendran V. Green synthesized ZnO nanoparticles against bacterial and fungal pathogens. Progress in Natural Science: Materials International. 2012;22(6):693-700.
69. Manjunath K, Ravishankar TN, Kumar D, Priyanka KP, Varghese T, Naika HR, et al. Facile combustion synthesis of ZnO nanoparticles using Cajanus cajan (L.) and its multidisciplinary applications. Materials Research Bulletin. 2014;57:325-34.
70. Shinde VV, Dalavi DS, Mali SS, Hong CK, Kim JH, Patil PS. Surfactant free microwave assisted synthesis of ZnO microspheres: Study of their antibacterial activity. Applied Surface Science. 2014;307:495-502.
71. Jan T, Iqbal J, Ismail M, Mansoor Q, Mahmood A, Ahmad A. Eradication of Multi-drug Resistant Bacteria by Ni Doped ZnO Nanorods: Structural, Raman and optical characteristics. Applied Surface Science. 2014;308:75-81.
72. Vijayakumar S, Arulmozhi P, Kumar N, Sakthivel B, Prathip Kumar S, Praseetha PK. Acalypha fruticosa L. leaf extract mediated synthesis of ZnO nanoparticles: Characterization and antimicrobial activities. Materials Today: Proceedings. 2020;23:73-80.
73. Chennimalai M, Do JY, Kang M, Senthil TS. A facile green approach of ZnO NRs synthesized via Ricinus communis L. leaf extract for Biological activities. Materials Science and Engineering: C. 2019;103:109844.
74.Susheela S., Sunil K., Bulchandini BD., Shalini T and Shelza B, 2013. Green synthesis of silver nanoparticles and their antimicrobial activity against gram positive and gram negative bacteria. Inter. J. Biotech. Bioeng. Res, 4:635-640.
75. Zhang Y, Gao X, Zhi L, Liu X, Jiang W, Sun Y, et al. The synergetic antibacterial activity of Ag islands on ZnO (Ag/ZnO) heterostructure nanoparticles and its mode of action. Journal of Inorganic Biochemistry.

2014;130:74-83.
76. Bai H, Liu Z, Sun DD. Hierarchical ZnO/Cu "corn-like" materials with high photodegradation and antibacterial capability under visible light. Physical Chemistry Chemical Physics. 2011;13(13):6205.
77. Li M, Zhu L, Lin D. Toxicity of ZnO Nanoparticles toEscherichia coli: Mechanism and the Influence of Medium Components. Environmental Science & Technology. 2011;45(5):1977-83.
78. Trease GE and Evan WC, 1983. Textbook of Pharmacognosy, Edition 12, English language Book society, Balliere Tindall, 309-315 and 706-708.
79. Kokate CK, Purohit AP and Ghokhale SB, 1997. Pharmacognosy, Nirali Prakashan, Pune, India.
80. Hegde Karunkar and Joshi Arun B, 2010. Preliminary phytochemical screening and antipyretic activity of Carissa spinarum root extract. Scholars Research Library Der Pharm. letter,, 2(3):255.